Accessing lithium−oxygen battery discharge products in their native environments via transmission electron microscopy grid electrode

Basak, Shibabrata; Baaij, Siemen; Ganapathy, Swapna; George, Chandramohan; Tempel, Hermann; Kungl, Hans; Kelder, Erik M.; Zandbergen, Henny W.; Wagemaker, Marnix; Eichel, Rüdiger A.

DOI
10.1021/acsaem.0c01803

Publication date
2020

Document Version
Final published version

Published in
ACS Applied Energy Materials

ACS APPLIED ENERGY MATERIALS

www.acsaem.org

Letter

Accessing Lithium−Oxygen Battery Discharge Products in Their Native Environments via Transmission Electron Microscopy Grid Electrode

Shibabrata Basak,* Siemen Baaij, Swapna Ganapathy, Chandramohan George, Hermann Tempel, Hans Kungl, Erik M. Kelder, Henny W. Zandbergen, Marnix Wagemaker, and Rüdiger-A. Eichel

Cite This: *ACS Appl. Energy Mater.* 2020, 3, 9509−9515

Read Online

ACCESS | Metrics & More | Article Recommendations | Supporting Information

ABSTRACT: High-fidelity and facile ex situ transmission electron microscopy (TEM) characterization of lithium−oxygen ($Li-O_2$) batteries is still limited by challenges in preserving the native environment of $Li-O_2$ discharge products. The extreme reactivity and moisture sensitivity of the discharge products means that they are quickly altered during sample retrieval from cycled batteries and transfer for TEM analysis, resulting in loss of original information. We here demonstrate that by using a TEM specimen grid directly in $Li-O_2$ batteries as both support electrode and sample collector overlaid on a standard oxygen diffusion electrode, discharge products that are formed on the grid can be kept pristine.

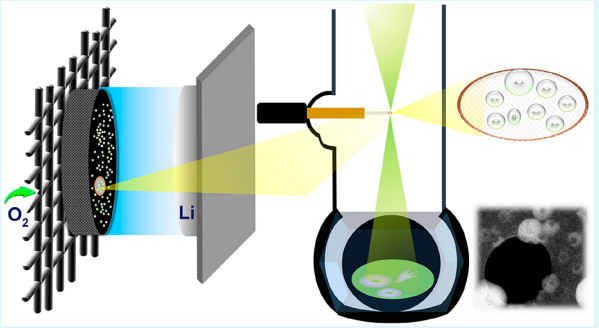

KEYWORDS: *Li−O_2 chemistries, electron microscopy, electrodes, carbon specimen grid and batteries*

Comprehensive understanding of high-energy battery chemistries underpinning their optimization is urgently needed for further aiding global electromobility via battery technologies. Among the many potential electrochemical storage chemistries being developed, lithium−oxygen ($Li-O_2$) batteries have been the focal point for battery researchers over the past decade,[1−3] because $Li-O_2$ features a high theoretical energy density of ∼3500 Wh/kg, which corresponds to an increase of about 1 order of magnitude of what today's Li-ion technology can provide at system level. Despite this potential, real-world $Li-O_2$ batteries at system level have not been built to date, because the complex $Li-O_2$ battery chemistry is plagued by many challenges at both fundamental and technology levels.[4−7] Particularly, the electrolyte used—either aqueous or nonaqueous—or the fuel-gas supply system—gas-open or closed-gas−catalyst/redox mediator supported or unsupported, in the presence of impurities (e.g., H_2O)—tends to alter the reaction courses leading to the formation of various discharge products (e.g., Li_2CO_3, Li_2O, LiOH, and Li_2O_2) and therefore impacts the practical energy/power capabilities and lifetime of these batteries, meaning that their actual deliverable performance can vary significantly (compared to their theoretical values when translating from cell to system level). A $Li-O_2$ battery is assembled with Li metal as anode and porous carbon as oxygen diffusion electrode, which are separated by an ion conducting membrane (e.g., cellgard, Whatman papers, and so on) soaked in with an electrolyte. The discharge cycle of a nonaqueous $Li-O_2$ battery involves the formation of Li_2O_2, which is then decomposed during charge according to the reaction $2Li^+ + O_2 + 2e^- \leftrightarrow Li_2O_2$ (∼3.0 V vs Li/Li^+).[3,6,8] This lithium peroxide formation via oxygen reduction reaction (ORR) and its decomposition via oxygen evolution reaction (OER) during charge−discharge cycling is the cornerstone of $Li-O_2$ battery chemistry, which determines capacity, longevity and round-trip efficiency of $Li-O_2$ batteries. The formation of discharge products are known either to occur via direct deposition at the porous cathode surface or to grow in the electrolyte before being precipitated on the porous electrode surface, and the occurrence of either of these depends on the effective donor number (DN) and acceptor number (AN) of the electrolyte used,[6,9,10] which is an indicator for the degree of solubility of discharge products in electrolytes (as solvent). For example, electrolytes with high DN promote the growth of more crystalline disk and toroidal shaped Li_2O_2 via solution-mediated growth, while low DN induces a passivation of carbon electrodes with amorphous Li_2O_2 film via surface-mediated growth, which typically results in electrode pore clogging and leading to diminished discharge capacity and premature battery failure.[9,10] Because the morphology and structure of discharge products are of crucial importance to the

Received: July 28, 2020
Accepted: September 25, 2020
Published: September 25, 2020

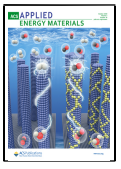

https://dx.doi.org/10.1021/acsaem.0c01803
ACS Appl. Energy Mater. 2020, 3, 9509−9515

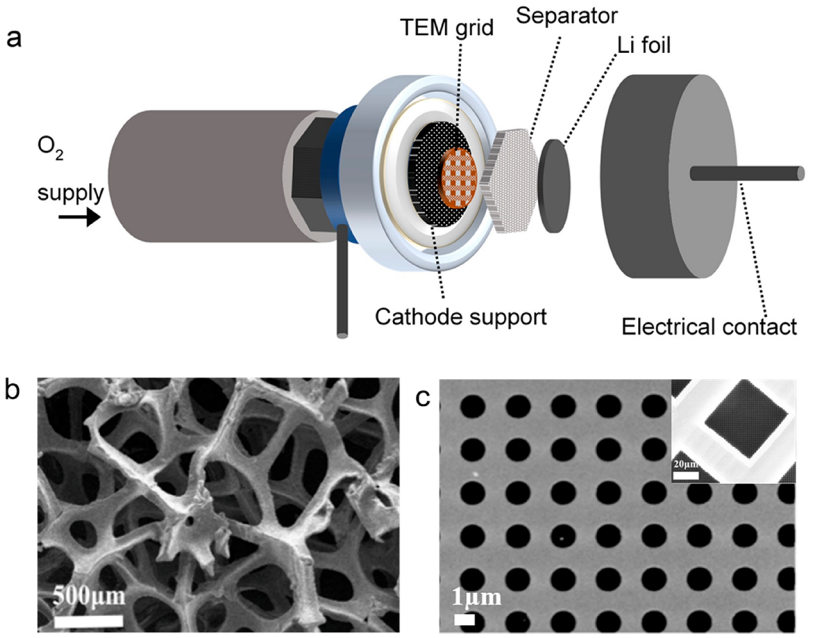

Figure 1. Schematic showing the use of conventional perforated TEM copper grid with holey carbon film as both support electrode and sample collector in Li−O_2 batteries: (a) the components of the Li−O_2 battery rig (custom-built)—a stainless steel mesh which allows O_2 introduction into the cell through porous carbon paper coated with active carbon slurry as cathode, on which a TEM grid is placed and lithium foil as anode is separated using separators soaked with electrolyte; (b) SEM image of a carbon porous electrode; (c) SEM images of the TEM grid showing the regular perforations in it.

operation, cycle life, and viability of Li−O_2 batteries, a wide range of spectroscopic and diffraction techniques have been employed to study the underlying mechanisms that dictate Li−O_2 battery cycling behavior in terms of ORR products.[11−13] While each of these provides valuable information on Li−O_2 electrode processes, much of the obtainable information is mostly about the whole electrode, i.e., the average electrochemical processes taking place across the electrochemically active sites of electrodes, meaning that the crucial details of local electrochemical processes involving intermediates at the nanoscale are not fully captured. Transmission electron microscopy (TEM) as a material characterization tool is routinely used to visualize local morphological, structural, and compositional information down to atomic scales and also to visualize battery electrode processes/products via either ex situ/postmortem analysis of cycled electrodes or in situ/operando investigation mainly using open-cell configuration with either ionic liquid or oxidized lithium or LiPON as electrolyte.[14−16] Although MEMS chips allow for the use of liquid electrolytes for in situ battery experiments,[17,18] electron beam even in low dosage generates considerable amount of solvated species during TEM imaging which can affect the inherent mechanism.[19,20] In theory, although these solvated species can be flushed out from the system by a continuous liquid flow, there is a prevailing doubt with regard to its (degree of) effectiveness. Unlike the traditional Li-ion batteries where only the transfer of Li-ions is mediated by electrolytes, the Li−O_2 electrode processes additionally rely on solvated species in electrolytes whose reactivities strongly influence the local Li−O_2 electrode processes and so the end results.[9,10] Because of these reasons, Li−O_2 battery characterization aimed at understanding the mechanistic processes of discharge products via operando TEM is not straightforward, with many possible outcomes that are mutually inclusive. Therefore, there is still a greater reliance on ex situ characterization approaches because (i) they allow for battery cycling in well-controlled electrochemical conditions so that discharge products can be terminated and investigated in desired charge/discharged states and (ii) the quality/state of discharge products can be varied depending on cycling conditions. Despite these advantages, ex situ TEM's applicability in studying the discharge products of Li−O_2 battery is limited by the many practical difficulties presented by the nature of Li−O_2 battery chemistry.

First, upon dismantling cycled batteries and scratching discharge products off Li−O_2 battery electrodes (for TEM sample preparation), reactions between discharge products and electrolyte and electrode support are already significant enough to alter the native environment. Use of the state-of-the-art TEM sample preparation methods using focused ion beam (FIB) is also limited as the Ga-ion beam tends to modify discharge products. On top of that the highly air/moisture sensitive nature of Li−O_2 discharge products further complicates the transfer of samples (from Ar/He filled glovebox to TEM via sample preparation and mounting), as even slight air exposure can potentially cause new features to be developed, thus masking as well as modifying the original Li−O_2 battery discharge products. Second, the instability of Li−O_2 discharge products during TEM imaging where the electron beam sensitivity of discharge products can trigger their disintegration or transformation while performing TEM measurements, giving rise to misleading information about Li−O_2 battery cycling products. While the issue of discharge products decomposition during TEM investigation can be somewhat mitigated by the combination of moderate acceleration voltage (e.g., 200 kV) and low electron beam dose in short exposure especially in scanning transmission electron microcopy (STEM) mode as described in our recent work,[21] the problem of Li−O_2 discharge products losing their actual chemical signatures and morphological features during TEM sample preparation is extremely challenging to date. Therefore, easily accessible and facile methods that are capable of preserving the pristine nature of discharge product during

https://dx.doi.org/10.1021/acsaem.0c01803
ACS Appl. Energy Mater. 2020, 3, 9509−9515

TEM sample preparation and transfer are still needed to support a whole range of TEM characterization, thus enabling high-fidelity local analysis of Li−O_2 battery discharge products in their original environments. In this report we show that conventional TEM grids with holey carbon film that are typically used as specimen substrates for general imaging purposes can be employed as electrodes in a custom-built rig (Figure 1), such that Li−O_2 chemistry can be performed directly on TEM grids by taking advantage of their similar geometry to that of a porous carbon oxygen diffusion electrode, which then can be reliably employed for post TEM analysis; thereby, the grids are always kept in protected environments for TEM analysis.

A typical electrode for Li−O_2 battery is prepared by casting carbon- or non-carbon-based active materials (with/without catalyst nanoparticles) onto a porous carbon paper/felt, which serves as oxygen diffusion cathode.[5,22,23] Figure 1a shows schematic of the rig used in our experiments, where a TEM grid is placed on top of a porous carbon electrode, which with a Li metal foil served as a Li−O_2 battery. Figure 1b shows an SEM image of such porous carbon (commercial) featuring an open pore network. On the other hand, TEM imaging grids are basically copper mesh on which a thin carbon-coated polymer film is laminated. Since the carbon films are perforated (Figure 1c), this combination of Cu mesh and holey carbon allows for the retention of thin samples and for direct transmission of electron beam (for imaging purposes). It can be noticed that this TEM grid with holey carbon is somewhat similar to that of the planar cross-section of a porous carbon paper typically used in a Li−O_2 cell (Figure 1b). Because of this, it is possible to employ TEM grids directly in place of porous carbon paper electrode and to perform Li−O_2 electrochemistry on it. The carbon film (on TEM grid) itself can act as an active material or the active material in the form of slurry can be added externally via drop-casting onto the grids to fabricate O_2 diffusion electrodes for TEM studies (the other electrode being Li metal) as shown in Figure 1. After cycling they can be removed at ease from the rig and transferred to a TEM holder, which is performed in an Ar filled glovebox using a vacuum transfer holder (Supporting Information). Previously, TEM Cu grids (with or without) carbon films have been employed for studying Li metal dendrites, which involved Li plating directly on TEM grids in coin type cells, followed by breaking battery to retrieve grids that were flash-frozen by liquid nitrogen.[24,25] But Li−O_2 battery studies via TEM grid present different issues, because, first, ensuring the discharge products formed on the TEM grid in appreciable densities is difficult and, second, it is imperative to establish that the discharge products formed on TEM holey carbon grids exhibit similar characteristics to that typically formed on the standard porous carbon paper (given the higher sensitivity of Li−O_2 chemistry). If these can be achieved, the direct use of TEM grids for studying Li−O_2 discharge products can then eliminate the need of strenuous sample preparation methods while retaining the native electrode environments. First, to compare the morphology of discharge products that can be formed on both types of electrodes, they were (carbon paper and TEM grid) coated with activated carbon slurry. More details of electrode preparation and Li−O_2 battery assembly can be found in the Supporting Information. These batteries with 1 M LiTFSi in TEGDME serving as electrolyte were discharged to 2.2 V vs Li/Li^+ at a current density of 50 $\mu A/cm^2$ (Figure S2). The discharge curve in terms of its voltage plateau is characteristic of ORR in a Li−O_2 cell. X-ray diffraction (XRD) patterns obtained from porous carbon confirm that the discharge products were indeed Li_2O_2 and can be found in Supporting Information (Figure S3). We then carefully compared the SEM images of both porous carbon electrode, Figure 2a,b, and the TEM grid, Figure 2c,d. In Figure 2c, the

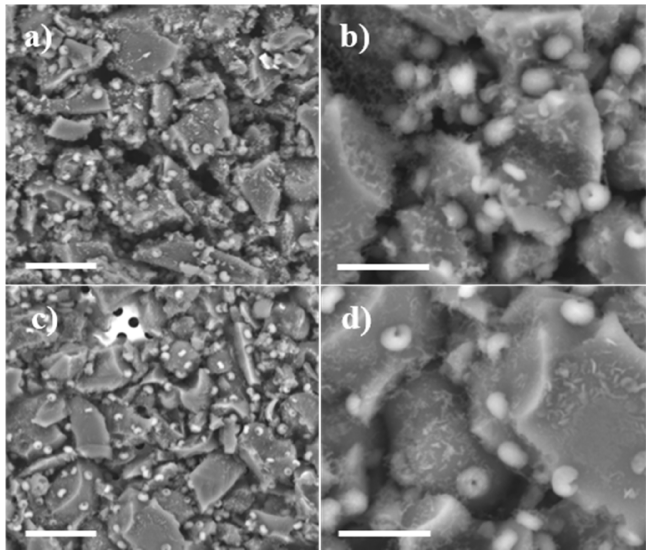

Figure 2. SEM images comparing the discharge products formed on active carbon coating at different magnifications: (a, b) on porous paper; (c, d) on TEM grid. Scale bar is 5μm.

holes on the TEM grids can be spotted through incomplete slurry coating. The appearance of identical donut shaped (toroidal) particles on both types of electrodes are characteristics of Li_2O_2 particles formed on a typical Li−O_2 battery discharge cycle. Scanning electron microscopic energy dispersive X-ray (SEM-EDX) mapping also highlights the oxygen-rich discharge products on the TEM grid as shown in Figure S4 of the Supporting Information. The results obtained on both types of electrodes are in line with literature, in particular those with the use of electrolyte (e.g., 1 M LiTFSi in TEGDME) having an intermediate donor number, which is known to trigger both solution-mediated and surface-mediated Li_2O_2 growth, especially at low current densities.[9,10] This shows that the TEM grid can perfectly act as both support electrode and sample collector with their pores (holes) enabling O_2 diffusion. Therefore, having a TEM grid alongside the traditional carbon electrode is the most effective way to capture/collect discharge products reliably onto TEM grids in densities suitable for further investigation, and the nature of discharge products formed on grids is the same as that of standard oxygen electrodes, obtained at full discharge capacities, which also eliminates any possibilities of grid influencing the course of reactions.

The next step was to explore whether the processes such as surface-meditated and solution-mediated growth of Li−O_2 discharge products can be studied comparatively by extending this grid approach, in such a way that relative distinctions between the two types of growth modes can be made. We therefore covered one-half of the TEM grid with 20 nm thick gold coating (for this the grids were placed under metal masks before e-beam evaporation). This gold coating can make this side of the grid electrically more conductive, while the other half of the grid still has carbon film which is not very conductive, and in this way it is possible to perform Li−O_2 chemistry on two different surfaces using the same TEM grid. It is known that gold

https://dx.doi.org/10.1021/acsaem.0c01803
ACS Appl. Energy Mater. 2020, 3, 9509−9515

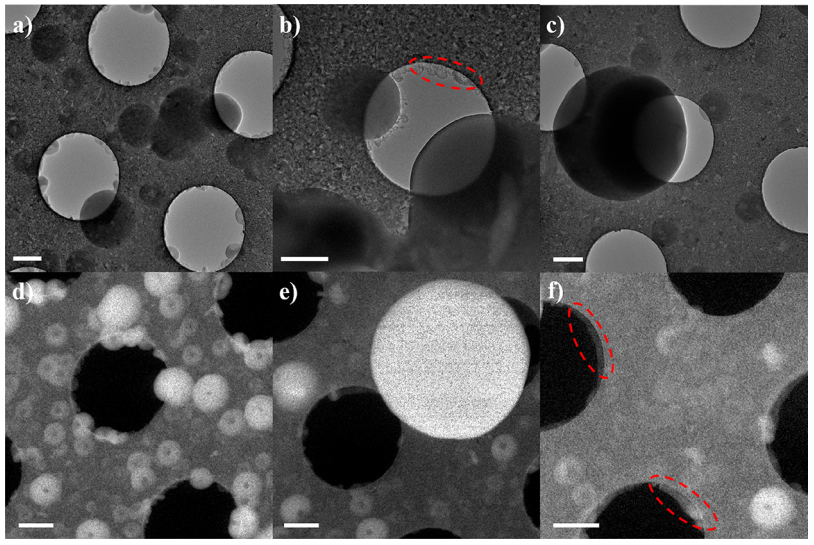

Figure 3. BF-TEM images showing discharge products formed at various locations on the gold coated part of TEM grid (a−c) and thickness map using EFTEM imaging (d−f). The scale bar is 500 nm.

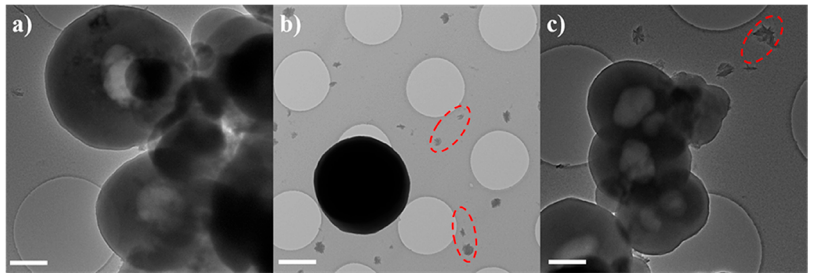

Figure 4. Discharge products formed at various locations on the non-gold-coated part of the TEM grid (a−c). The scale bar is 500 nm.

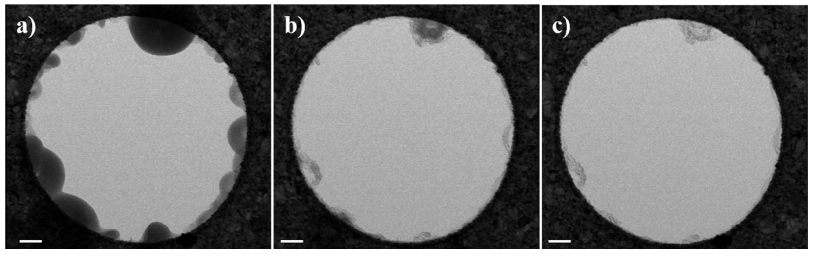

Figure 5. Electron beam induced lithium peroxide transformation/disappearance at dose rate of 89 (e/Å^2)/s (a) at initial time, (b) after 90 s, and (c) after 180 s exposure. The scale bar is 200 nm.

does not actually act as a catalyst aiding the formation of Li_2O_2 but tends to provide stability to Li−O_2 batteries (by minimizing electrolyte decomposition and avoiding CO_2 formation).[10] Thus, the gold coating of electrodes does not necessarily alter the local electrochemistry in terms of discharge products but may influence the deposition pathways of discharge products. The cell containing a porous carbon paper (coated with active carbon slurry) along with a TEM grid (this time is not coated with active slurry but half the part of the grid coated with gold) is discharged to 2.2 V at a current density of 50 μm/cm^2. Figure 3 shows the discharge product formed at various locations of the gold-coated areas of the grid. From the bright field TEM images (Figure 3a−c) and energy filtered TEM (EFTEM) thickness maps (Figure 3d−f), performed with 10 eV slit, three distinct size variations in the discharge products can be observed, which are randomly shaped deposition (>20 nm) around the edges of the holes (marked with red dotted lines), large particles (with a size range of ∼100−600 nm) throughout the grid, and a few very large sized particles (>1 μm) randomly on the grid. Figure S5 in the Supporting Information shows the selected area diffraction pattern (SAED) and electron energy loss spectra (EELS) of the random shaped discharge product formed around the hole, which demonstrate that these lithium containing discharge products are amorphous in nature. Thickness maps of particles (Figure 3d−f) reveal their donut shapes (toroidal), which are a typical morphology of Li−O_2 battery discharge products.[26,27] On the other hand, Figure 4 shows the discharge product formed at various locations of a grid without gold coating, where most of the discharge products are seemingly of one size with a particle size > 1 μm, which are also typical of Li−O_2 discharge products in terms of their shape. But the appearance of some flake-like discharge products as in Figure 4b is very surprising and has not been observed before under similar conditions. This could possibly be the very early stages of discharge products growth.

https://dx.doi.org/10.1021/acsaem.0c01803
ACS Appl. Energy Mater. 2020, 3, 9509−9515

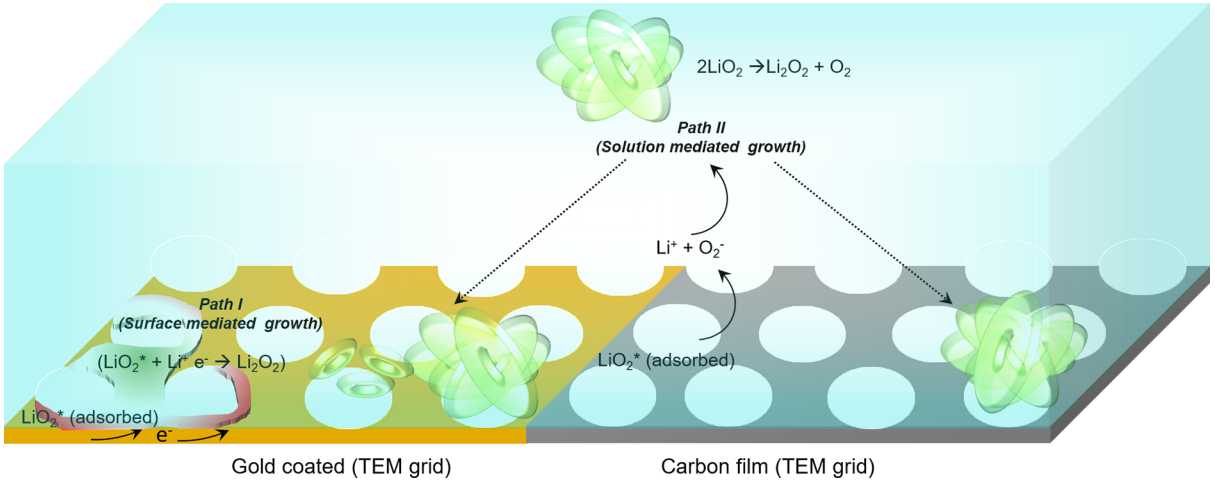

Figure 6. Schematic showing discharge product formation pathways at highly electron conductive substrate (gold-coated part) and poorly electron conductive substrate (noncoated part) during oxygen reduction reaction in medium donor number electrolytes.

However, the beam sensitivity of the sample restricted recording reliable oxygen core loss spectra, as recording O K-edge requires either long exposure time (~5 s in TEM mode with ~100 (e/Å^2)/s dose rate) or long dwell time (in STEM mode). Since the size of flakes is very small, their rapid degradation under electron beam can be observed in Figure 5. Therefore, those flakes are assumed to be the discharge products consisting of LiO_2, although it was not characterized fully by EELS (O K-edge), which in fact needs more sophisticated imaging conditions, for example, the use of fast detectors, and is recommended for future studies.

Although our study is to mainly demonstrate that TEM grid electrodes are a viable solution to further characterize the complex Li−O_2 chemistry in their native environments, we summarized the above observations, which is schematically presented in Figure 6, in an attempt to rationalize why the discharge products formed at the different parts of the TEM grid (gold coated and noncoated) are apparently different (given that gold here is not a catalyst but a better electron conductor). We therefore considered different possible pathways for the formation of discharge products.

As discussed earlier, given that the medium donor number electrolyte (1 M LiTFSi in TEGDME) used in this study can induce both surface mediated growth and solution mediated growth. LiO_2^*(adsorbed), formed according to $LiO_2^* \leftrightarrow Li^+ + O_2^-$,[9,10] requires an electron supply from the surface to undergo a single electron reduction, forming film-like amorphous discharge product, resulting in surface-mediated growth. On the gold-coated part of the grid, this process can proceed readily due to better electronic conductivity of the surface (via path *I* as in Figure 6). However, after initial deposition, the electronic contact is significantly removed because Li_2O_2 is an insulator. On the non-gold-coated part of the grid with a thin layer of amorphous carbon, this reaction side has limited electron conductivity, indicating that a one electron reduction step may not be as good as the gold-coated surface; therefore, this should favor the reverse of the above reaction, leading to solution-mediated growth, through which discharge products can form at the electrode surface,[9,28] according to $2LiO_2 \rightarrow Li_2O_2 + O_2$, where the growth occurs in solution followed by deposition at the electrode surface via disproportion. Because this does not rely entirely on electronic contribution from the electrode surface, it is therefore equally probable for both a gold-coated and a noncoated surface.

On the noncoated surface (Figure 4) the particles mostly were >1 μm, alongside some small flake-like particles, whereas a small random deposition at the edge of the holes and medium (100−600 nm) as well as big particles (>1 μm) can be seen on the gold-coated part as in Figure 3. Therefore, the small amorphous deposition at the edges of the holes (Figure 3) is most likely a result of surface-mediated growth (*path I*), which may be facilitated by better electron conductivity of the gold surface. We note that these types of growths also occur throughout the gold-coated part but cannot be observed easily from the TEM images due to the presence of the gold coating (high-*Z* contrast material) underneath the discharge products. Since the batteries (containing the porous carbon support electrodes with activated carbon) were discharged for ~40 h, solution-mediated growth resulted in large and different sized Li_2O_2 particles that are evident on both gold-coated and noncoated parts of the grid (*path II*). However, more detailed work is required to understand why smaller toroids were not observed on the noncoated surface under these conditions. Since the small flakes on the noncoated surface were not characterized via EELS due to their high e-beam sensitivity, we did not include that in Figure 6.

Similar results were obtained when we replaced the half-gold-coated grid with either a fully gold coated or nongold coated grid. Also, when we had used only the grids (without the porous carbon support electrode), toroid shaped Li_2O_2 were not formed, due to the limited capacity of batteries; therefore it is recommended that TEM grids be used alongside the carbon support electrodes in order to collect representative discharge products onto grids.

Despite this ability to visualize the initial stages of discharge products which is critical to the understanding of the Li−O_2 battery mechanism, this calls for more systematic works on discharge products under various electrochemical conditions, e.g., different stages of discharge at different current densities and overpotentials which are known to produce Li_2O_2 having different structures and morphologies[29,30] and more elaborate imaging conditions and analysis. Using this grid approach from revisiting the previously established mechanisms based on the use of ORR catalysts to the state-of-the-art Li−O_2 batteries that make use of redox mediators, a better understanding of Li−O_2

https://dx.doi.org/10.1021/acsaem.0c01803
ACS Appl. Energy Mater. 2020, 3, 9509−9515

chemistries can be established. This method is particularly suitable for identifying whether parasitic discharge products, e.g., Li_2CO_3, are formed regardless of their structure and morphology. This method can also be extended to investigate other metal−air chemistries (Na−air, Zn−air, and Mg−air, etc.) in terms of the nature of discharge products formed on different active materials.

In conclusion, loss of details about the surroundings of the discharge products and lack of preservation of the pristine discharge product during the cycled Li−O_2 battery sample preparation are the two major problems, limiting the application of TEM in Li−O_2 battery research. We have shown that using conventional holey carbon TEM grids alongside porous carbon as cathode, discharge products formed on the TEM grid are established to be identical with that of the standard carbon electrodes, providing electrode samples for high-fidelity TEM studies. We have also shown the TEM grid can be used to distinguish as well as analyze solution-mediated and surface-mediated Li_2O_2 deposition. This method to preserve the native environment of Li−O_2 electrode processes together with its simplicity can facilitate widespread use of TEM for better understanding of Li−O_2 reaction mechanism toward the realization of real-world Li−O_2 batteries.

■ ASSOCIATED CONTENT

Supporting Information

(PDF). The Supporting Information is available free of charge at https://pubs.acs.org/doi/10.1021/acsaem.0c01803.

Methods section; figures and graphs regarding experiments (PDF)

Movie S1 showing degradation of the discharge product under electron beam. (AVI)

■ AUTHOR INFORMATION

Corresponding Author

Shibabrata Basak − *Department of Applied Sciences, Delft University of Technology, Delft 2628CJ, The Netherlands; Institute of Energy and Climate Research, Fundamental Electrochemistry (IEK-9), Forschungszentrum Jülich GmbH, Jülich 52425, Germany;* orcid.org/0000-0002-4331-4742; Email: s.basak@fz-juelich.de

Authors

Siemen Baaij − *Department of Applied Sciences, Delft University of Technology, Delft 2628CJ, The Netherlands*

Swapna Ganapathy − *Department of Radiation Science and Technology, Delft University of Technology, Delft 2629JB, The Netherlands*

Chandramohan George − *Dyson School of Design Engineering, Imperial College London, London SW7 2AZ, United Kingdom;* orcid.org/0000-0003-2906-6399

Hermann Tempel − *Institute of Energy and Climate Research, Fundamental Electrochemistry (IEK-9), Forschungszentrum Jülich GmbH, Jülich 52425, Germany*

Hans Kungl − *Institute of Energy and Climate Research, Fundamental Electrochemistry (IEK-9), Forschungszentrum Jülich GmbH, Jülich 52425, Germany*

Erik M. Kelder − *Department of Radiation Science and Technology, Delft University of Technology, Delft 2629JB, The Netherlands*

Henny W. Zandbergen − *Department of Applied Sciences, Delft University of Technology, Delft 2628CJ, The Netherlands*

Marnix Wagemaker − *Department of Radiation Science and Technology, Delft University of Technology, Delft 2629JB, The Netherlands;* orcid.org/0000-0003-3851-1044

Rüdiger-A. Eichel − *Institute of Energy and Climate Research, Fundamental Electrochemistry (IEK-9), Forschungszentrum Jülich GmbH, Jülich 52425, Germany; Institute of Physical Chemistry, RWTH Aachen University, Aachen 52074, Germany;* orcid.org/0000-0002-0013-6325

Complete contact information is available at: https://pubs.acs.org/10.1021/acsaem.0c01803

Notes

The authors declare no competing financial interest.

■ ACKNOWLEDGMENTS

This work was financially supported by NWO NANO Project 11498 and BMBF Projects—CatSE (Project 13XP0223A) and LiSi (Project 13XP0224B). C.G. acknowledges funding from the Royal Society, London for an URF (Grant UF160573).

■ REFERENCES

(1) Peng, Z.; Freunberger, S. A.; Chen, Y.; Bruce, P. G. A Reversible and Higher-Rate Li-O2 Battery. *Science (Washington, DC, U. S.)* **2012**, *337* (6094), 563−566.

(2) Liu, T.; Leskes, M.; Yu, W.; Moore, A. J.; Zhou, L.; Bayley, P. M.; Kim, G.; Grey, C. P. Cycling Li-O2 Batteries via LiOH Formation and Decomposition. *Science (Washington, DC, U. S.)* **2015**, *350* (6260), 530−533.

(3) Xia, C.; Kwok, C. Y.; Nazar, L. F. A High-Energy-Density Lithium-Oxygen Battery Based on a Reversible Four-Electron Conversion to Lithium Oxide. *Science (Washington, DC, U. S.)* **2018**, *361* (6404), 777−781.

(4) Feng, N.; He, P.; Zhou, H. Critical Challenges in Rechargeable Aprotic Li-O2 Batteries. *Adv. Energy Mater.* **2016**, *6* (9), 1502303.

(5) Yang, S.; He, P.; Zhou, H. Research Progresses on Materials and Electrode Design towards Key Challenges of Li-Air Batteries. *Energy Storage Mater.* **2018**, *13*, 29−48.

(6) Liu, T.; Vivek, J. P.; Zhao, E. W.; Lei, J.; Garcia-Araez, N.; Grey, C. P. Current Challenges and Routes Forward for Nonaqueous Lithium-Air Batteries. *Chem. Rev.* **2020**, *120*, 6558.

(7) Wandt, J.; Jakes, P.; Granwehr, J.; Gasteiger, H. A.; Eichel, R.-A. Singlet Oxygen Formation during the Charging Process of an Aprotic Lithium-Oxygen Battery. *Angew. Chem.* **2016**, *128* (24), 7006−7009.

(8) Li, Z.; Ganapathy, S.; Xu, Y.; Zhu, Q.; Chen, W.; Kochetkov, I.; George, C.; Nazar, L. F.; Wagemaker, M. Fe_2O_3 Nanoparticle Seed Catalysts Enhance Cyclability on Deep (Dis)charge in Aprotic Li−O_2 Batteries. *Adv. Energy Mater.* **2018**, *8* (18), 1703513.

(9) Johnson, L.; Li, C.; Liu, Z.; Chen, Y.; Freunberger, S. A.; Ashok, P. C.; Praveen, B. B.; Dholakia, K.; Tarascon, J. M.; Bruce, P. G. The Role of LiO2 Solubility in O2 Reduction in Aprotic Solvents and Its Consequences for Li-O 2 Batteries. *Nat. Chem.* **2014**, *6* (12), 1091−1099.

(10) Kwak, W. J.; Rosy; Sharon, D.; Xia, C.; Kim, H.; Johnson, L. R.; Bruce, P. G.; Nazar, L. F.; Sun, Y. K.; Frimer, A. A.; Noked, M.; Freunberger, S. A.; Aurbach, D. Lithium-Oxygen Batteries and Related Systems: Potential, Status, and Future. *Chem. Rev.* **2020**, *120*, 6626−6683.

(11) Gittleson, F. S.; Ryu, W. H.; Taylor, A. D. Operando Observation of the Gold-Electrolyte Interface in Li-O2 Batteries. *ACS Appl. Mater. Interfaces* **2014**, *6* (21), 19017−19025.

(12) Lim, H.; Yilmaz, E.; Byon, H. R. Real-Time XRD Studies of Li-O 2 Electrochemical Reaction in Nonaqueous Lithium-Oxygen Battery. *J. Phys. Chem. Lett.* **2012**, *3* (21), 3210−3215.

(13) Ganapathy, S.; Adams, B. D.; Stenou, G.; Anastasaki, M. S.; Goubitz, K.; Miao, X.; Nazar, L. F.; Wagemaker, M. Nature of Li 2 O 2

Oxidation in a Li − O 2 Battery Revealed by Operando. *J. Am. Chem. Soc.* **2014**, *136*, 16335−16344.
(14) Basak, S.; Migunov, V.; Tavabi, A. H.; George, C.; Lee, Q.; Rosi, P.; Arszelewska, V.; Ganapathy, S.; Vijay, A.; Ooms, F.; Schierholz, R.; Tempel, H.; Kungl, H.; Mayer, J.; Dunin-Borkowski, R. E.; Eichel, R.-A.; Wagemaker, M.; Kelder, E. M. Operando Transmission Electron Microscopy Study of All-Solid-State Battery Interface: Redistribution of Lithium among Interconnected Particles. *ACS Appl. Energy Mater.* **2020**, *3*, 5101−5106.
(15) Basak, S.; Ganapathy, S.; Malladi, S. K.; Vicarelli, L.; Schreuders, H.; Dam, B.; Kelder, E. M.; Wagemaker, M.; Zandbergen, H. W. Designing Reliable Operando TEM Experiments to Study (De)-Lithiation Mechanism of Battery Electrodes. *J. Electrochem. Soc.* **2019**, *166* (14), A3384−A3386.
(16) Yuan, Y.; Amine, K.; Lu, J.; Shahbazian-Yassar, R. Understanding Materials Challenges for Rechargeable Ion Batteries with in Situ Transmission Electron Microscopy. *Nat. Commun.* **2017**, *8* (May), 1−14.
(17) Gu, M.; Parent, L. R.; Mehdi, B. L.; Unocic, R. R.; McDowell, M. T.; Sacci, R. L.; Xu, W.; Connell, J. G.; Xu, P.; Abellan, P.; Chen, X.; Zhang, Y.; Perea, D. E.; Evans, J. E.; Lauhon, L. J.; Zhang, J. G.; Liu, J.; Browning, N. D.; Cui, Y.; Arslan, I.; Wang, C. M. Demonstration of an Electrochemical Liquid Cell for Operando Transmission Electron Microscopy Observation of the Lithiation/Delithiation Behavior of Si Nanowire Battery Anodes. *Nano Lett.* **2013**, *13* (12), 6106−6112.
(18) Holtz, M. E.; Yu, Y.; Gunceler, D.; Gao, J.; Sundararaman, R.; Schwarz, K. A.; Arias, T. A.; Abruña, H. D.; Muller, D. A. Nanoscale Imaging of Lithium Ion Distribution during in Situ Operation of Battery Electrode and Electrolyte. *Nano Lett.* **2014**, *14* (3), 1453−1459.
(19) de Jonge, N.; Houben, L.; Dunin-Borkowski, R. E.; Ross, F. M. Resolution and Aberration Correction in Liquid Cell Transmission Electron Microscopy. *Nat. Rev. Mater.* **2019**, *4* (1), 61−78.
(20) Abellan, P.; Mehdi, B. L.; Parent, L. R.; Gu, M.; Park, C.; Xu, W.; Zhang, Y.; Arslan, I.; Zhang, J. G.; Wang, C. M.; Evans, J. E.; Browning, N. D. Probing the Degradation Mechanisms in Electrolyte Solutions for Li-Ion Batteries by in Situ Transmission Electron Microscopy. *Nano Lett.* **2014**, *14* (3), 1293−1299.
(21) Basak, S.; Jansen, J.; Kabiri, Y.; Zandbergen, H. W. Towards Optimization of Experimental Parameters for Studying Li-O2 Battery Discharge Products in TEM Using in Situ EELS. *Ultramicroscopy* **2018**, *188*, 52−58.
(22) Ganapathy, S.; Li, Z.; Anastasaki, M. S.; Basak, S.; Miao, X. F.; Goubitz, K.; Zandbergen, H. W.; Mulder, F. M.; Wagemaker, M. Use of Nano Seed Crystals to Control Peroxide Morphology in a Nonaqueous Li-O2 Battery. *J. Phys. Chem. C* **2016**, *120* (33), 18421−18427.
(23) Ganapathy, S.; Heringa, J. R.; Anastasaki, M. S.; Adams, B. D.; Van Hulzen, M.; Basak, S.; Li, Z.; Wright, J. P.; Nazar, L. F.; Van Dijk, N. H.; Wagemaker, M. Operando Nanobeam Diffraction to Follow the Decomposition of Individual Li2O2 Grains in a Nonaqueous Li-O2 Battery. *J. Phys. Chem. Lett.* **2016**, *7* (17), 3388−3394.
(24) Zachman, M. J.; Tu, Z.; Choudhury, S.; Archer, L. A.; Kourkoutis, L. F. Cryo-STEM Mapping of Solid−Liquid Interfaces and Dendrites in Lithium-Metal Batteries. *Nature* **2018**, *560* (7718), 345−349.
(25) Wang, J.; Huang, W.; Pei, A.; Li, Y.; Shi, F.; Yu, X.; Cui, Y. Improving Cyclability of Li Metal Batteries at Elevated Temperatures and Its Origin Revealed by Cryo-Electron Microscopy. *Nat. Energy* **2019**, *4* (8), 664−670.
(26) Lu, Y. C.; Gallant, B. M.; Kwabi, D. G.; Harding, J. R.; Mitchell, R. R.; Whittingham, M. S.; Shao-Horn, Y. Lithium-Oxygen Batteries: Bridging Mechanistic Understanding and Battery Performance. *Energy Environ. Sci.* **2013**, *6* (3), 750−768.
(27) Yu, W.; Wang, H.; Hu, J.; Yang, W.; Qin, L.; Liu, R.; Li, B.; Zhai, D.; Kang, F. Molecular Sieve Induced Solution Growth of Li2O2 in the Li-O2 Battery with Largely Enhanced Discharge Capacity. *ACS Appl. Mater. Interfaces* **2018**, *10* (9), 7989−7995.
(28) Aurbach, D.; McCloskey, B. D.; Nazar, L. F.; Bruce, P. G. Advances in Understanding Mechanisms Underpinning Lithium-Air Batteries. *Nat. Energy* **2016**, *1* (9), 1−11.
(29) Ganapathy, S.; Adams, B. D.; Stenou, G.; Anastasaki, M. S.; Goubitz, K.; Miao, X. F.; Nazar, L. F.; Wagemaker, M. Nature of Li2O2 Oxidation in a Li-O2 Battery Revealed by Operando X-Ray Diffraction. *J. Am. Chem. Soc.* **2014**, *136* (46), 16335−16344.
(30) Adams, B. D.; Radtke, C.; Black, R.; Trudeau, M. L.; Zaghib, K.; Nazar, L. F. Current Density Dependence of Peroxide Formation in the Li−O2 Battery and Its Effect on Charge. *Energy Environ. Sci.* **2013**, *6* (6), 1772−1777.

https://dx.doi.org/10.1021/acsaem.0c01803
ACS Appl. Energy Mater. 2020, 3, 9509−9515